International Journal of Heat and Mass Transfer 52 (2009) 1443–1450

Contents lists available at ScienceDirect

International Journal of Heat and Mass Transfer

journal homepage: www.elsevier.com/locate/ijhmt

On-line temperature measurements for polymer thermal conductivity estimation under injection molding conditions

R. Le Goff [a], D. Delaunay [a,*], N. Boyard [a], Y. Jarny [a], T. Jurkowski [a], R. Deterre [b]

[a] Université de Nantes, Nantes Atlantique Universités, Laboratoire de Thermocinétique de Nantes, UMR CNRS 6607, La Chantrerie, rue Christian Pauc, BP 50609, 44306 Nantes Cedex 3, France
[b] Université de Nantes, Nantes Atlantique Universités, Laboratoire OPERP, 2 avenue Professeur Jean Rouxel, 44475 Carquefou Cedex, France

ARTICLE INFO

Article history:
Received 4 February 2008
Received in revised form 5 July 2008
Available online 13 December 2008

Keywords:
Thermal conductivity
Semi-crystalline polymers

ABSTRACT

The determination of reliable and accurate values of thermal conductivity of semi-crystalline polymers is a challenging task because of the intimate coupling existing between crystallization and the conditions of molding process. In this paper, we describe an experimental device that allows to the molding of the polymer and to submit it to conditions close to those of the injection process (high pressure and shear). It permits to identify the thermal conductivity according to the temperature, both in melted and solid phases by solving an inverse heat conduction problem. Taking into account the shrinkage of the piece and its anisotropy, our results demonstrate that this conductivimeter is a reliable experimental apparatus.

1. Introduction

The thermal conductivity is one of the essential parameters to predict with accuracy the temperature in a thermoplastic polymer part during molding. It is also a parameter for which the scattering of the results is the most important. Hieber [1] presents a comparison between a large number of data from nine different teams using various experimental techniques to measure the thermal conductivity of the isotactic polypropylene (PP) between −160 °C [2] and 300 °C [3–6]. One can note a wide scattering, at atmospheric pressure, of the values in the solid state in the range [40 °C, 120 °C] since they vary between 0.18 and 0.27 W/m K. In the melted phase, the measurement is not easy and the values vary between 0.13 and 0.22 W/m K in the range [160 °C, 300 °C]. Such scattering is directly linked to the one of the temperature field, which has strong consequences on the thermal phenomena analysis. The reasons of this scattering are difficult to understand; one can discuss the semi-crystalline nature of the solid material and the morphology, which can induce some discrepancies. Indeed, Galeski et al. [7] studied the conductivity in spherolites and show that the anisotropy induced by the crystalline structure on the one hand and the difference of conductivity between the amorphous and crystalline phases on the other hand. Therefore, according to the processing conditions of the sample, a given polymer will be able to present different thermal conductivities because of the crystallinity [8,9] and even of the crystalline orientation. This is confirmed by Dai and Tanner [10] who show that the anisotropy of conductivity in a PP subjected to shear is the result of oriented crystallization driven by the flow (which can lead to shear) during the filling of the molding cavity. The observation of the oriented structure development of PP submitted to shear is done using in situ small- and wide-angle X-ray scattering (SAXS and WAXS, respectively) [11,12]. Consequently, the measurement of the conductivity must be done under conditions as close as possible of the processing conditions to reproduce the shearing and must be systematically related to the crystallinity. In the domain of transformation, the measures must be considered with caution since the crystallized fraction evolves. Different models are available to express the thermal conductivity according to the crystallized fraction and are compared by Legoff et al. [13]. They give very close results considering the relatively weak thermal contrast existing between the crystalline and amorphous phases.

Confronted to the lack of adapted apparatus [14], we designed an experimental device to estimate thermal conductivity, which enables to mold the polymer and to submit it to conditions near of those of the injection molding (high pressure and shear). This mold is equipped with a specific instrumentation to identify the thermal conductivity as a function of temperature, both in melted and solid phases by solving an inverse heat conduction problem. This method of analysis requires to know with accuracy the initial temperature field in the polymer, and to make the measurements in a thick piece where heat transfers are correctly modeled (i.e. adequacy of the model).

It is shown in this paper, how this inverse approach associated to a specific experimental apparatus called "on-line conductivime-

* Corresponding author. Tel.: +33 (0)2 40 68 31 11; fax: +33 (0)2 40 68 31 41.
E-mail address: didier.delaunay@univ-nantes.fr (D. Delaunay).

0017-9310/$ - see front matter © 2008 Elsevier Ltd. All rights reserved.
doi:10.1016/j.ijheatmasstransfer.2008.07.053

Nomenclature

Bi	Biot number
Cov	covariance matrix
C_p	specific heat (J/kg K)
e	thickness (m)
F_a	anisotropy factor
JM	number of parameters
NF	number of time steps
R_V	volumetric shrinkage
R_e	shrinkage along the thickness
r	correlation coefficient
Rtc	thermal contact resistance (m^2 K/W)
Rtc_0	initial Rtc (m^2 K/W)
t	time (s)
T	temperature (K)
V	specific volume (m^3/kg)
w	descent direction
X	sensitivity

Greek symbols

α	conversion degree
γ	descent length
λ	thermal conductivity (W/m K)
ϕ_{losses}	heat flux losses (W/m^2)
ρ	density (kg/m^3)
σ	standard deviation

Subscripts

a	amorphous
cp	central plate
pol	polymer
sc	semi-crystalline
surf	surface of the mold

ter" is validated by determining the thermal conductivity of a very well characterized polymer (polypropylene HV252).

2. Description of the apparatus

The principle of the conductivimeter is based on the injection and the cooling of a melted polymer within two identical cylindrical cavities (thickness = 3.9×10^{-3} m), separated by a metallic central plate. As shown in Fig. 1, the polymer is sandwiched between the central plate and two symmetrical heat exchangers. A heat flux sensor instruments each of these exchangers and thermocouples are implanted in the middle of the central plate. Temperatures within the polymer are quite difficult to measure, especially with thermocouples, during the injection and the cooling of the melted polymer. From our experience and because of the internal stresses induced by the crystallization, it is impossible to avoid the displacements of micro-thermocouples. Therefore, measuring the temperature of the central plate has a significant advantage: it behaves as a capacitive thermocouple with a very well defined geometry, and it is easy to take into account its heat capacity in the sensor model equations. Therefore, this temperature plate measurement is available as additional data for developing the solution of the inverse heat conduction problem.

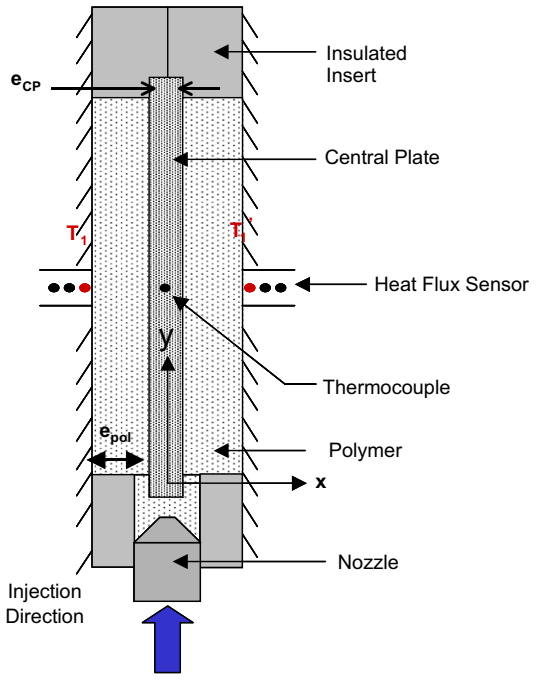

Fig. 1. Cutaway view of the conductivimeter device.

An originality of our molding conditions consists in heating the mold before the injection step. This enables to start cooling after the end of injection. Electrical resistances heat the mold and are designed so that the initial temperature is as uniform as possible in the molding cavities. After injection, a gas flowing in the heat exchangers is used for cooling. Two heat flux sensors measure the heat flow extracted from the molding cavities. Each of these measurements results of the inverse analysis of the data given by three micro-thermocouples (Tc_i, $i = 1,2,3$). These sensors are not invasive since their constitutive material and their surface roughness are similar to those of the mold. In addition, a system of hot channels maintains the polymer in the melted state in the feeding circuit and the mold is equipped with a heated nozzle.

The removable central plate is maintained by two insulating polymer rings resisting to high temperature. These rings act as lateral walls of the molding cavities and limit the heat losses in the radial direction. The central plate is equipped with a rubber-molded tail that avoids the melted polymer to flow outside the molding cavities, and allows the connection of the thermocouple wires. Four thermocouples, placed in the periphery of the central plate, enable the estimation of the heat losses. Their fabrication is described in a previous work [15].

During the cooling step of the injection cycle, the metallic plate can be considered as a capacitive temperature sensor placed in the heart of the polymer. The value of the Biot number, which defines the ratio between the internal resistance of the plate ($=e/2\lambda$) and the thermal contact resistance Rtc between the metal and the polymer (estimated to 5×10^{-4} m^2 K W^{-1}), is close to $Bi = 0.05$. the assumption of a capacitive model equation is then valid.

A view of the mold is presented in Fig. 2. Before injection, the mold and the molding cavities are heated to the injection temperature of the polymer and the cooling is triggered after filling. The electrical heaters impose a homogeneous initial temperature.

3. Data acquisition example

Fig. 3 presents a characteristic example of experimental recorded data, which will be used to identify the thermal conductivity. The parameters of the injection process are specified in Table 1.

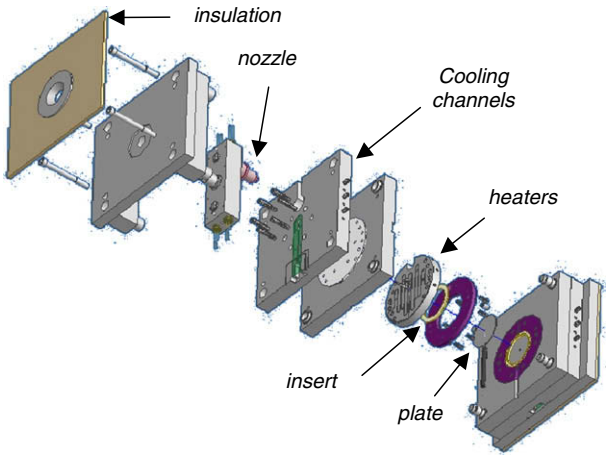

Fig. 2. Detail of the whole mold.

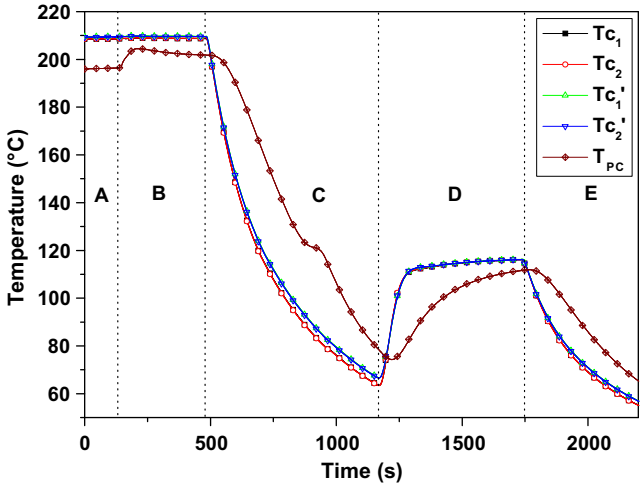

Fig. 3. Measured temperatures on the central plate and in the molding cavity.

Table 1
Injection conditions for PP HV252

Injection parameters	Experimental values
Injection temperature	210 °C (493 K)
Mold temperature	210 °C (493 K)
Injection time	10 s
Holding pressure before cooling	20 MPa
Holding pressure during cooling	Atmospheric pressure

The objective of such experiment is to get information on the temperatures of the material in both melted and solid phases. These measurements are then used to calculate the thermal conductivity of the injected material as a function of temperature. In order to uncouple the temperature from the crystallization phenomenon, a first cooling is carried out until the complete solidification of the piece. Then, this one is heated until a temperature below the melting point of the polymer. Finally, the solid piece is cooled again.

Fig. 3 displays the five temperatures measured by the first two thermocouples Tc_1 and Tc_2 located in the flux sensor no. 1, by the first two thermocouples Tc'_1 and Tc'_2 in the flux sensor no. 2 and finally by the thermocouple located in the central plate T_{PC}.

Before the injection, part A highlights a difference of about 8 K between the temperature of the wall of the molding cavities and the temperature in the middle of the central plate.

Part B corresponds to the injection and the setting in regime of the mold/polymer assembly. Due to the injection of the melted polymer, the temperature of the central plate increases and then decreases slightly. It reveals the influence of heat losses in the central plate. Thus, before the cooling of the piece, a quasi-steady regime is waited for.

Part C shows the evolution of the temperatures during cooling. They are quasi-symmetrical on both sides of the cavities. The cooling process is not fast enough to observe significant differences between the temperatures given by the first two thermocouples of the heat flux sensor. We therefore considered a spatially uniform temperature in the metallic part of the mold near the surface of the molding cavities. We can also notice a plateau of temperature ($T \approx 120$ °C) measured by the thermocouple of the central plate. It corresponds to the heat release induced by the crystallization of the polymer.

Part D presents the heating of the piece up to 115 °C, i.e. to a temperature lower than the melting temperature of PP. The heat losses in the central plate are still visible by the difference of temperature between the cavity walls and the core of the mold.

Finally, in part E, the solid polymer piece is cooled.

4. Direct problem formulation

Let us consider the example corresponding to Fig. 3. The applied thermal cycle provides information on the temperature of the polymer during two distinct phases: the melted phase ($\alpha = 0$) and the solid phase ($\alpha = 1$). Fig. 4 represents the temperature intervals, for each phase, that are used to estimate the thermal conductivity of the polymer. It is important to note that some precautions must be taken in melted state in order to insure that the polymer does not begin to solidify on the walls of the molding cavity. To estimate the thermal conductivity with $\alpha = 0$, the temperature interval has to be selected in order to avoid starting crystallization in the piece. Thus, a model of crystallization [13] helps us to know when the solidification starts at the piece surface.

The estimation of the thermal conductivity when $\alpha = 0$ or $\alpha = 1$ (no crystallization model is then required), is performed by solving an inverse heat conduction problem. It is based on a direct non-linear heat conduction model without source term according to the following system of equations:

In the polymer

$$\rho_{pol}(T)Cp_{pol}(T)\frac{\partial T}{\partial t} = \frac{\partial}{\partial x}\left(\lambda_{pol}(T)\frac{\partial T}{\partial x}\right), \quad 0 < x < e_{pol} \tag{1a}$$

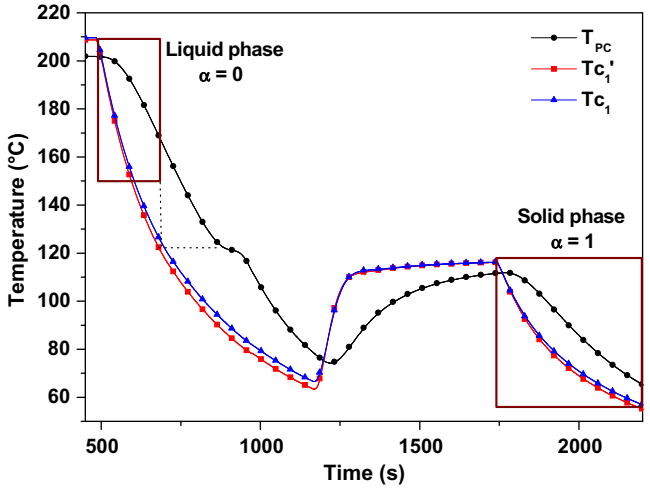

Fig. 4. Domain of temperature processed for the evaluation of the conductivity.

In the central plate

$$\rho_{CP}Cp_{CP}\frac{e_{CP}}{2}\frac{\partial T_{CP}}{\partial t} = -(\phi_{pol} + \phi_{losses}) \tag{1b}$$

Boundary conditions

$$\lambda_{pol}(T)\frac{\partial T}{\partial x}\bigg|_{x=e_{pol}} = \phi_{pol} = \frac{T_{CP} - T_{x=e_{pol}}}{Rtc} \tag{2}$$

$$T_{surf}(t) = \frac{Tc_1(t) + Tc_1'(t)}{2} \tag{3a}$$

$$-\lambda_{pol}(T)\frac{\partial T}{\partial x}\bigg|_{x=0} = \frac{T_{surf} - T_{x=0}}{Rtc} \tag{3b}$$

Initial condition

$$T(x=0, t=0) = T_{surf}(t=0), \quad 0 < x < e_{pol} \tag{4}$$

where ϕ_{pol} is the heat flux given to the polymer by the central plate and ϕ_{losses} is the heat flux lost by the central plate.

The mold is assumed to be symmetrical with respect to the central plate. The boundary condition (Eq. (2)) corresponds to the heat flux coming from the central plate. The heat losses ϕ_{losses}, already discussed in [13], are estimated to be constant during the time interval considered for the thermal conductivity estimation and is equal to $\approx$2500 W/m^2 (i.e. a total heat loss of 0.6 W, which is very small in comparison of the total heat flux of 55 W through the surface of the sample). The methodology for its determination has been explained in a previous publication [13]. At the walls of the molding cavities, the boundary condition (Eq. (3a)) is given by the experimental average temperature (calculated from Tc_1 and Tc_1').

To take into account the thermal effect of shrinkage during cooling, thermal resistances varying with time have to be considered [16]. They also depend on the process conditions [17]. The total thermal resistance (Eqs. (5a) and (5b)) is calculated from the shrinkage $R_e(t)$ associated to the thickness (Eq. (5c))

$$Rtc(t) = Rtc_0 \text{ if } \Delta V = 0 \tag{5a}$$

$$Rtc(t) = \frac{R_e(t)e_{pol}}{\lambda_{air}} \text{ if } \Delta V \neq 0 \quad \text{and } Rtc(t) > Rtc_0 \tag{5b}$$

where λ_{air}, the average thermal conductivity of air in the temperature range of cooling, is equal to 0.027 W/m K. Rtc_0, the thermal contact resistance between the material and the mold, is estimated to 6×10^{-4} m^2 K/W [13,16,18], for the studied PP in the melted state and 1.7×10^{-3} m^2 K/W in the solid state [13]. ΔV is the volume variation induced by the temperature decrease. ΔV remains $\approx$0 as long as the gate is not frozen (shrinkage is compensated by the packing pressure).

We consider an identical shrinkage on each side of the part. The volumetric shrinkage (noted $R_V(t)$) anisotropy is taken into account through an anisotropy factor F_a, which distributes the shrinkage in the thickness and in the plane of the sample. Luyé [19] estimates the shrinkage anisotropy of the PP for a 3 mm thick piece. He determines that F_a varies between 1.74 and 1.61 depending on the holding pressure. In our case, one finds that the factor of anisotropy is between 1.6 and 1.7

$$R_e(t) = \frac{R_V(t)}{F_a} \tag{5c}$$

$$R_V(t) = \frac{\Delta V}{V_0} \tag{5d}$$

$R_V(t)$ is calculated for each time step from specific volume expressions (see Section 5), i.e. Eq. (19) for the melted (amorphous) state and Eq. (20) for the solid (semi-crystalline) state.

5. Description of the inverse method

Let us recall that the inverse parameter estimation consists in minimizing the deviation between measured temperatures and calculated ones through the solving of the heat conduction equations. This difference is called criterion or objective function. In our case, the variations of the thermal conductivity versus temperature is described under the shape of a vector $\boldsymbol{\lambda} = [\lambda_1, \ldots, \lambda_j, \ldots, \lambda_{JM}]^T$, with JM components, associated to an a priori given temperature table $\mathbf{T} = [T_1, \ldots, T_j, \ldots, T_{JM}]^T$. Between two values T_j and T_{j+1} the conductivity is assumed to be linear.

The least-square criterion to be minimized, takes the form of following equation:

$$J(\boldsymbol{\lambda}) = \frac{1}{2}\sum_{n=1}^{NF}(T(x=0, t_n; \boldsymbol{\lambda}) - T_{CP}(t_n))^2 \tag{6}$$

where NF is the number of sampling times.

The structure of the method, illustrated in Fig. 5, is based on an iterative algorithm. For each iteration, the vector to identify is corrected up to the convergence of the criterion toward a ε value, which is chosen depending on the variance of the measurement noise. The inverse algorithm for heat conduction problem has already been studied and used [20]. It requires the computation of the gradient $\nabla J(\boldsymbol{\lambda})$ of the criterion. The influence of the initial parameter vector on the estimated solution is usually studied by running the optimization algorithm for different initial values. In practice, it is assumed that a range of 0.15–0.35 W/m K is typical for the thermal conductivity of such polymer, and the algorithm was initialized with the mean value of this interval. In order to increase the convergence rate of the minimization process, we chose the conjugated gradient method. It consists in computing at each iteration, γ^{iter} the descent depth, and w_j^{iter} the descent direction, according to Eqs. (7)–(9)

$$\lambda_j^{iter+1} = \lambda_j^{iter} + \gamma^{iter} \cdot w_j^{iter} \tag{7}$$

Descent direction:

$$w_j^{iter} = -\nabla J_j^{iter} + \beta^{iter} w_j^{iter-1} \tag{8}$$

with

$$\beta^{iter} = \frac{\left\|\nabla J^{iter}\right\|^2}{\left\|\nabla J^{iter-1}\right\|^2}$$

Descent depth:

$$\gamma^{iter} = -\frac{\left\langle \nabla J^{iter}, w^{iter} \right\rangle}{\left\| X^{iter} w^{iter} \right\|^2} \tag{9}$$

We mention that the descent depth (Eq. (9)), is not optimal for such non-quadratic optimization problem, and convergence is not always guaranteed. Nevertheless, it is necessary to determine

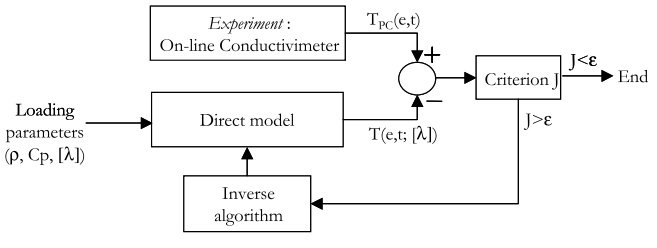

Fig. 5. Structure of the resolution of an inverse problem.

whether the estimation is possible and with which accuracy. In this context, we achieved a sensitivity analysis of the temperature measurement to the unknown parameters, which have to be estimated. This analysis generally indicates whether minimization is possible or not. The coefficients of sensitivity $X_j(t,\lambda_j)$ are given by Eq. (10). They are defined by the first derivative of the temperature at the sensor location with respect to each parameter λ_j. It is similar to analyse the effect of a small perturbation $\delta\lambda_j$ on the temperature field

$$X_j(t,\lambda_j) = \frac{\partial T(e_{pol},t;\lambda_j)}{\partial \lambda_j} = \lim_{\delta\lambda_j \to 0} \frac{T(e_{pol},t;\lambda_j+\delta\lambda_j) - T(e_{pol},t;\lambda_j)}{\delta\lambda_j} \quad (10)$$

Assuming that the measurement errors are additive and have a constant standard deviation, the sensitivity matrix X can be used to calculate the covariance matrix (Eq. (11)) related to the estimation of λ

$$\mathrm{Cov}(\lambda) = \sigma^2 (X^{\mathrm{T}}X)^{-1} \quad (11)$$

where σ is the standard deviation of the measurement noise.

The diagonal terms of $\mathrm{Cov}(\lambda)$ correspond to the variance $\sigma^2_{\lambda j}$ of each parameter. Each non-diagonal term corresponds to each covariance between the parameters and permits to assess the correlation [21]. So the covariance matrix (Eq. (12)) enables to calculate the standard deviation of the estimation errors and the correlation coefficient noted r between two parameters according to Eq. (13):

$$\mathrm{Cov}(\lambda) = \begin{pmatrix} \sigma^2_{\lambda_1} & \mathrm{Cov}(\lambda_1,\lambda_2) \\ \mathrm{Cov}(\lambda_1,\lambda_2) & \sigma^2_{\lambda_2} \end{pmatrix} \quad (12)$$

$$r = \frac{\mathrm{Cov}(\lambda_1,\lambda_2)}{\sigma_{\lambda_1}\sigma_{\lambda_2}} \quad (13)$$

It is also interesting to determine the relative error on each parameter. It is usefull to appreciate the quality of the inversion independently of the magnitude (Eq. (14))

$$re_{\lambda_j} = \frac{\sigma_{\lambda_j}}{\lambda_j} \quad (14)$$

The method of estimation of thermal conductivity is validated on the HV252 polypropylene provided by SOLVAY®. This PP was the object of numerous studies within our laboratory; that's why its thermal properties are well known [13,22–24]. The models of the evolution of the heat capacity and the specific volume are given by the following equations:

$$Cp_{pol}(\alpha,T) = \alpha Cp_{sc}(T) + (1-\alpha)Cp_a(T) \quad (15)$$

$$V_{pol}(\alpha,T) = \alpha V_{sc}(T) + (1-\alpha)V_a(T) \quad (16)$$

To identify the specific heat $Cp_{sc}(T)$ and $Cp_a(T)$ in each phase of the polymer, DSC experiments were performed. Heat capacity is modeled using a linear relation versus the temperature in the following equations:

$$Cp_a = 3.10T + 2124 \quad \text{with } T \text{ in } ^\circ\mathrm{C} \quad (17)$$

$$Cp_{sc} = 10.68T + 1451 \quad (18)$$

The specific volume is deduced from PvT diagrams for which Fulchiron et al. published a reference paper [22]. In our case, specific volume is given by the following equations:

$$V_a = 1.138 + 6.773 \times 10^{-4}T \quad \text{with } T \text{ in } ^\circ\mathrm{C} \quad (19)$$

$$V_{sc} = 1.077 + 4.225 \times 10^{-4}T \quad (20)$$

Let us discuss the estimation the thermal conductivity in the solid phase, $\alpha = 1$. The temperature vector, associated to the conductivity vector, is chosen within the domain presented in Fig. 6. The conductivity can be estimated in the temperature range scanned by the central plate thermocouple. However, in order to cover the whole temperature domain, it is necessary to choose the minimal and maximal temperatures of the experiment as lower and upper boundary limits. We chose $T_{max} = 116\ ^\circ\mathrm{C}$ and $T_{min} = 55\ ^\circ\mathrm{C}$.

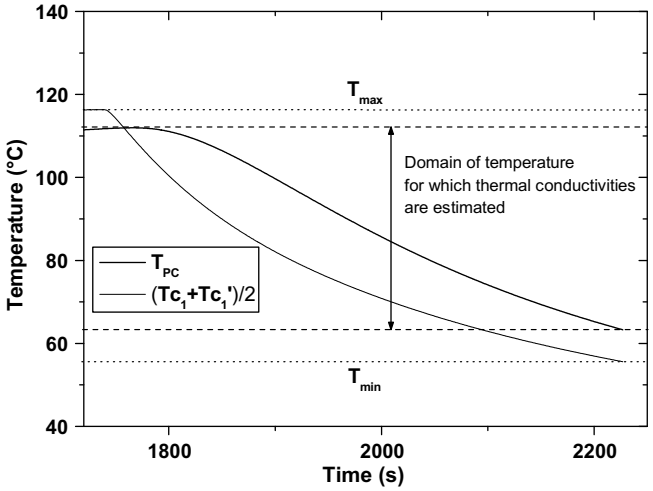

Fig. 6. Selection of the temperature domain for the evaluation of the thermal conductivity.

Fig. 7 presents the variations of the sensitivity coefficients versus time calculated in a configuration with JM = 7 parameters. Table 2 gives the principle of temperature parameterization of the thermal conductivity vector. The sensitivity coefficients have the same order of magnitude and are not correlated. Each parameter influences the domain of temperature close to the temperature for which it is defined. It means that the identification of the parameters is possible and accurate. However, Jarny and Maillet[21] note that in the evaluation of a function ($\lambda_{pol}(T)$ in our case), the sensitivity coefficients amplitudes decrease and get closer to each other when the number of parameters to estimate increases. It is due to the fact that each parameter relates to a smaller temperature interval, thereby reducing its impact on this one. Besides,

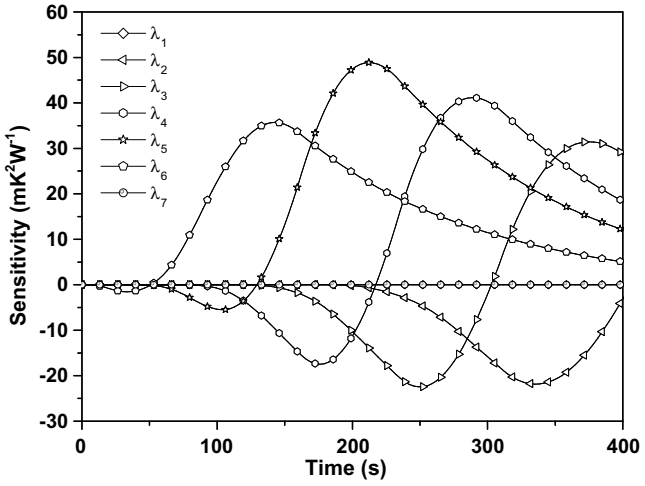

Fig. 7. Sensitivity in solid phase for a vector conductivity with JM = 7 components.

Table 2
λ parameterization vector

$[\lambda]$	λ_1	λ_2	λ_3	λ_4	λ_5	λ_6	λ_7
T (°C)	116 (T_{max})	110	96	86	76	66	55 (T_{min})

in the case of two too close parameters, their correlation is higher and the relative error on each parameter as well. On the other way, if the number of parameters of λ is lower, the assumption of linearity of the thermal conductivity between two temperatures becomes much stronger.

Eq. (21) presents the correlation matrix (always in the case of an identification of seven parameters). The standard deviation of the noise of measure is equal to 0.05 K

$$r(\lambda) = \begin{array}{c} \begin{matrix} \lambda_2 & \lambda_3 & \lambda_4 & \lambda_5 & \lambda_6 \end{matrix} \\ \begin{pmatrix} 1 & 0.54 & 0.74 & 0.18 & 0.18 \\ - & 1 & 0.16 & 0.37 & -0.008 \\ - & - & 1 & -0.27 & 0.35 \\ - & - & - & 1 & -0.65 \\ - & - & - & - & 1 \end{pmatrix} \end{array} \begin{matrix} \lambda_2 \\ \lambda_3 \\ \lambda_4 \\ \lambda_5 \\ \lambda_6 \end{matrix} \quad (21)$$

It appears more clearly that some parameters are rather highly correlated. For example, the parameter λ_2 is closely linked to λ_3 and λ_4, which can harm to its determination. The question of the number of parameters is then raised. In order to verify the influence of these correlations on the quality of the inversion, we draw the relative errors for each parameter (Fig. 8) given by Eq. (14). The maximum is obtained for the parameter λ_2, and is equal to 0.40%, which is very low. Thus, despite of some rather high correlation factors, the quality of the evaluation will not be affected.

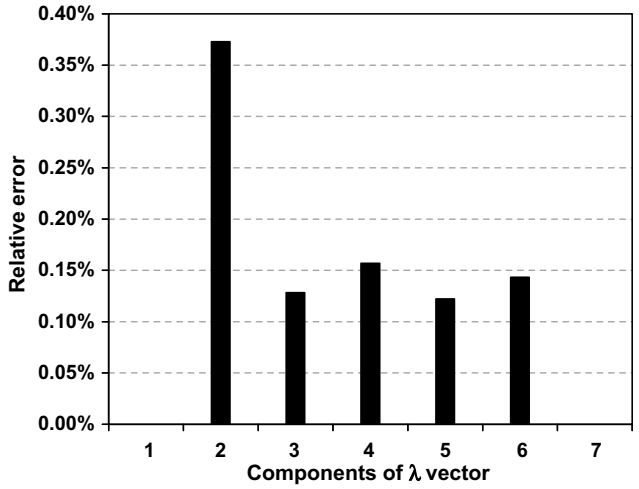

Fig. 8. Relative error due to measurement noise on the components of the estimated vector.

It is now necessary to quantify other sources of estimation error, especially those due to the input parameters assumed to be exactly known in the model equations, and those resulting of the initial guess in the iterative process. Additional calculations and sensitivity analysis were then performed. Fig. 9 presents the relative errors caused by a 10% error (this value is typical and acceptable for many thermal–physical parameters) on the heat flux losses, the heat capacity and density, and the initial guess. The highest errors are due to the uncertainties on the density and the specific heat. An error of 10% implies a mean error of ≈10% on the estimation of the thermal conductivity. Error on the flux losses has a little impact. The choice of the initial parameter has an influence only on the evaluation of the components near the beginning of the cooling. It should be also underlined that the errors due to measurement noise are of an order of magnitude lower than the errors due to the known parameters.

Considering these results, one can now estimate the conductivities of the PP in both melted and solid phases. Fig. 10a and b presents the evolutions of the square root of the criterion weighted by the number of time steps (i.e. $(J/NF)^{0.5}$) and the residuals (deviation between experimental and calculated temperatures of the central plate) for solid PP. The residuals depicted in Figs. 10b and 11b are the time varying deviations between the measured and the computed temperatures, at the end of the optimization process, after the final iteration (no. 15 for Fig. 10b, no. 20 for Fig. 11b). The minimum is reached at the end of 10 iterations and the residuals are less than 2σ of the measurement noise, except in the beginning of the cooling. This difference is due to the difficulty to take into account accurately the heat losses in the early times in the calculation of the temperature field.

The analysis of the sensitivities to the parameters estimated in liquid phase, give similar results to the analysis in the solid phase. We identified the values of the thermal conductivity for five temperatures. The criterion and the residuals for experiments in the liquid state of PP are also depicted in Fig. 11a and b. The criterion also converges toward a minimum in 10 iterations. The domain of temperature of the thermal conductivity identified being narrow since the influence of the heat flux losses on the residuals is more important. We suppress the thermal conductivities estimated in the domain where the residual are high because the measurements are biased.

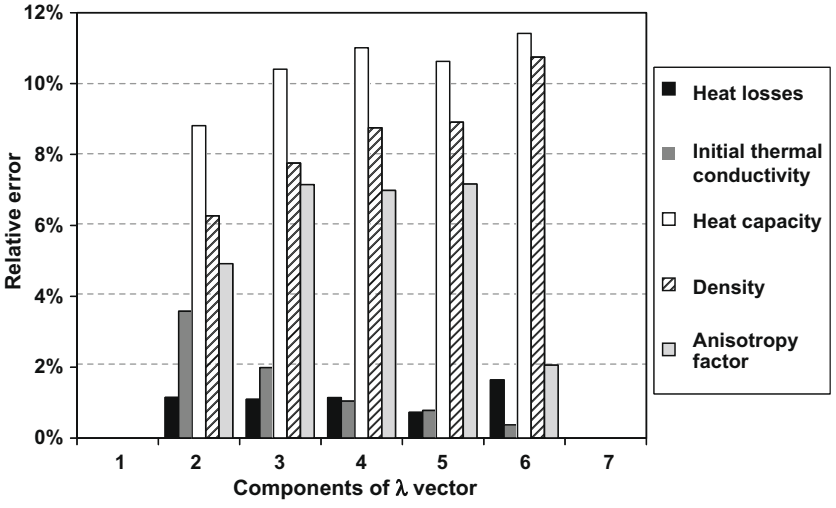

Fig. 9. Relative error on the components of the estimated vector due to a 10% relative error on the flux losses, the initial parameter and the thermal properties.

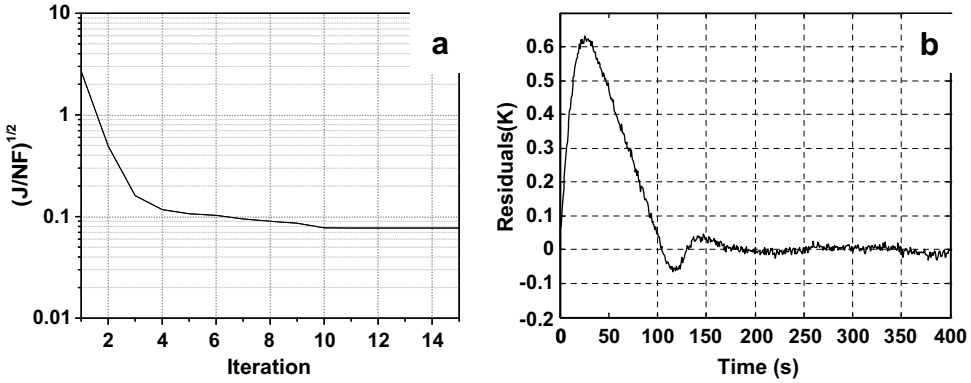

Fig. 10. Evolution of the *J* criterion (a) and residuals (b) for the evaluation of the thermal conductivity in solid phase.

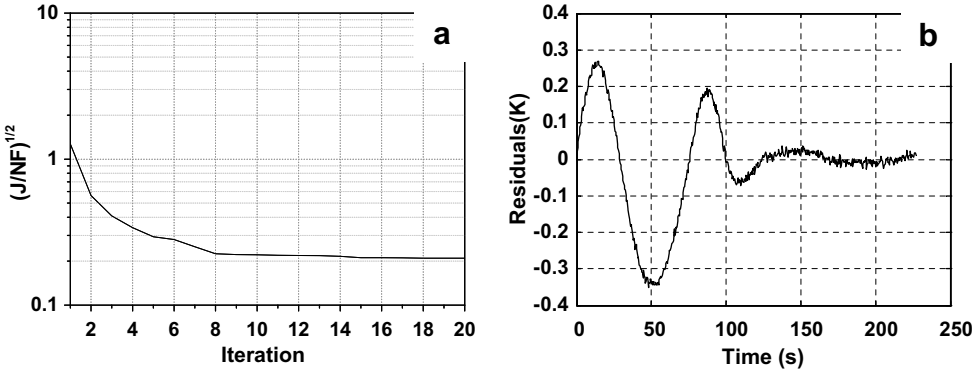

Fig. 11. Evolution of the *J* criterion (a) and residuals (b) in the evaluation of the thermal conductivity in liquid phase.

Fig. 12 summaries the results of the evaluation of the thermal conductivity in both melted phase and solid phases. They are presented in parallel of the measures performed with a hot guarded plate and of the interpolation made by Le Bot [25] on his own measurements. The results obtained in solid phase by our inverse method are satisfactory. They agree very well with the values obtained with the guarded hot plate apparatus. However, they underestimate the results of Le Bot for the lowest temperatures. In liquid phase, the thermal conductivity is estimated close to the one given by Le Bot (measured by shock probe [25]) within a margin of error of 5%.

In the melted state, our results agree with those of Lobo et al. [3] provided by a shock probe (same method than [25]). For the solid state, we recover the results of Gobé et al. (see [1]) determined by steady state concentric cylinders. Our transient method gives therefore values of conductivities in good agreement with those obtained with two steady state methods.

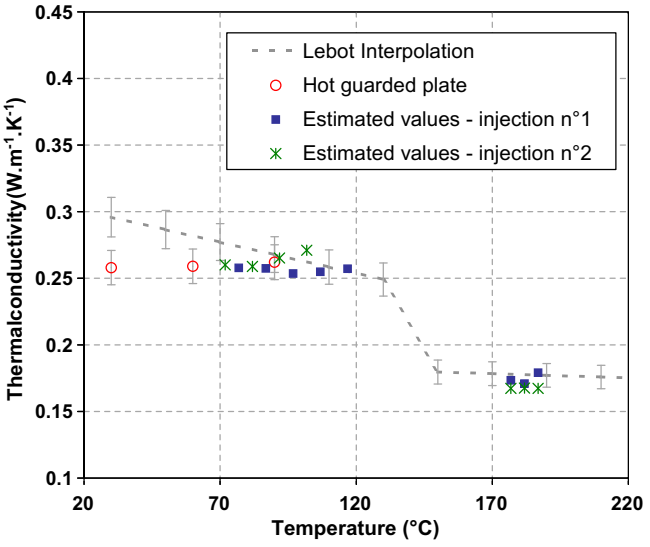

Fig. 12. Comparison between the identified thermal conductivities, the measures in hot plate and the results of Le Bot [25].

6. Conclusion

We propose a new experimental device and an associated data treatment to estimate the conductivity of semi-crystalline polymers in processing conditions. Shear effect and rapid crystallization are then taken into account and the estimation is performed on a representative sample. Our results are close to those presented in the literature, provided that the crystallinity is the same. This is not necessarily the case and it is a major relevant factor to explain the scattering of the measurements. In identical conditions of processing, our results are consistent with those made with a hot guarded plate. Our method requires nonetheless the introduction of the specific heat as well as the specific volume according to the temperature and possibly of the pressure as input data. We have to consider that the crystallization of the polymer generates a specific volume variation and more accurately shrinkage of the part, which therefore induce the apparition of an air gap. It is then taken in account by an equivalent thermal contact resistance. The anisotropy of the shrinkage adds an additional difficulty for the evaluation of the conductivity. Finally, a sensitivity analysis indicates that the esti-

mated properties are strongly influenced by the values of the thermal–physical properties of the polymer (C_p, ρ) compared to those of heat losses or initial guess λ.

A modification of the mold is currently in progress to ensure a constant contact between the walls of the mold and the injected sample.

Acknowledgments

This work was supported by Region des Pays de la Loire authority within the framework of pluri-annual grant and by FISH Program with Moldflow®, Legrand® and Solvay® partners. The authors thank Nicolas Lefevre and Luc Douillard for their crucial technical contribution.

References

[1] C.A. Hieber, Modeling/simulating the injection molding of isotactic polypropylene, Polym. Eng. Sci. 42 (7) (2002) 1387–1409.
[2] R.C. Steere, Detection of polymer transitions by measurement of thermal properties, J. Appl. Polym. Sci. 10 (1966) 1673–1685.
[3] H. Lobo, R. Newman, Thermal Conductivity of Polymers at High Temperatures and Pressures. SPE-ANTEC Technical Papers, second ed., vol. 36, Society of Plastics Engineers, 1990, pp. 862–865.
[4] D. Hands, Thermal transport properties of polymers, Rubber Chem. Technol. 50 (3) (1977) 480–522.
[5] C.L. Yen, H.C. Tseng, Y.Z. Wang, K.H. Hsieh, Thermal conductivity of glass fiber reinforced polypropylene under high pressure, J. Appl. Polym. Sci. 42 (5) (1991) 1179–1184.
[6] J.C. Ramsey III, A.L. Fricke, J.A. Caskey, Thermal conductivity of polymer melts, J. Appl. Polym. Sci. 17 (5) (1973) 1597–1605.
[7] A. Galeski, P. Milczarek, M. Kryszewski, Heat conduction in a two-dimensional spherulite, J. Polym. Sci. 15 (1977) 1267–1281.
[8] C.L. Choy, K. Young, Thermal conductivity of semi-crystalline polymers – a model, Polymer 18 (1977) 769–776.
[9] N. Sombatsomcop, A.K. Wood, Measurement of thermal conductivity of polymers using an improved Lee's disc apparatus, Polym. Test. 16 (1997) 203–223.
[10] S.C. Dai, R.I. Tanner, Anisotropic thermal conductivity in sheared polypropylene, Rheol. Acta 45 (2006) 228–238.
[11] A. Nogales, B.S. Hsiao, R.H. Somani, S. Srinivas, A.H. Tsou, F.J. Balta-Calleja, T.A. Ezquerra, Shear-induced crystallization of isotactic polypropylene with different molecular weight distributions: in situ small- and wide-angle X-ray scattering studies, Polymer 42 (2001) 5247–5256.
[12] R.H. Somani, B.S. Hsiao, A. Nogales, S. Srinivas, A.H. Tsou, I. Sics, F.J. Balta-Calleja, T.A. Ezquerra, Structure development during shear flow-induced crystallization of *i*-PP: in situ small- and wide-angle X-ray scattering studies, Macromolecules 33 (2000) 9385–9394.
[13] R. Legoff, G. Poutot, D. Delaunay, R. Fulchiron, E. Koscher, Study and modeling of heat transfer during the solidification of semi-crystalline polymers, Int. J. Heat Mass Transfer 48 (2005) 5417–5430.
[14] T. Jurkowski, D. Delaunay, Y. Jarny, Estimation of thermal conductivity of thermoplastic under molding conditions. An apparatus and an inverse algorithm, Int. J. Heat Mass Transfer 40 (1997) 4169–4181.
[15] H. Masse, E. Arquis, D. Delaunay, S. Quilliet, P.H. Le Bot, Heat transfer with mechanically driven thermal contact resistance at the polymer–mold interface in injection molding of polymers, Int. J. Heat Mass Transfer 47 (2004) 2015–2027.
[16] J.C. Yu, J.E. Sunderland, C. Poli, Thermal contact resistance in injection molding, Polym. Eng. Sci. 30 (24) (1990) 1599–1606.
[17] J.A. Hall, W.H. Ceckler, E.V. Thompson, Thermal properties of rigid polymers. I. Measurement of thermal conductivity and question concerning contact resistance, J. Appl. Polym. Sci. 33 (1987) 2029–2039.
[18] A. Bendada, A. Derdouri, M. Lamontagne, Y. Simard, Analysis of thermal contact resistance between polymer and mold in injection molding, Appl. Therm. Eng. 24 (2004) 2029–2040.
[19] J.F. Luyé, Etude thermophysique du refroidissement du polypropylène injecté, Thèse de doctorat, ENSAM de Paris, 1999.
[20] O.M. Alifanov, Inverse Heat Conduction, III-posed Problems, Wiley–Interscience, New York, 1985.
[21] Y. Jarny, D. Maillet, Problèmes inverses et estimation de grandeurs en thermique, Eurotherms Winter.
[22] R. Fulchiron, E. Koscher, G. Poutot, D. Delaunay, G. Régnier, Analysis of the pression effect on the crystallization kinetics of polypropylene: dilatometric measurements and thermal gradients modelling, J. Macromol. Sci. Phys. 40 (3–4) (2001) 297–314.
[23] D. Delaunay, P. Le Bot, R. Fulchiron, J.F. Luyé, G. Régnier, nature of contact between polymer and mold in injection molding. Part I. Influence of a non-perfect thermal contact, Polym. Eng. Sci. 40 (7) (2000) 1682–1691.
[24] D. Delaunay, P. Le Bot, R. Fulchiron, J.F. Luyé, G. Régnier, nature of contact between polymer and mold in injection molding. Part II. Influence of mold deflection on pressure history and shrinkage, Polym. Eng. Sci. 40 (7) (2000) 1692–1700.
[25] P. Le Bot, Comportement thermique des semi-cristallins injectés – application à la prediction des retraits, Thèse de doctorat, Université de Nantes, 1998.